Journal of Education, Science and Engineering
Vol 2 No. 1, 2026: 219-228
https://ojs.universityedu.org/index.php/jese/index
Online ISSN: 3122-019X || Print ISSN: 3122-0118

Static Performance of Compliant Vertical Access Risers Applied to Deepwater Floating Production System

Solomon Chukwuka Nwigbo
Department of Mechanical Engineering, Nnamdi Azikiwe University, Awka, Nigeria.
TETFUND Centre for Biotechnology, Engineering and Agricultural Translation Studies (TCE-Beats), Nnamdi Azikiwe University, Awka, Nigeria.

Tochukwu Chukwuka Oraelosi
Department of Mechanical Engineering, Nnamdi Azikiwe University, Awka, Nigeria

Sunday Madubueze Ofochebe
Department of Mechanical Engineering, Nnamdi Azikiwe University, Awka, Nigeria;

Obiora B. Ezeudu
Department of Civil Engineering, University of Victoria, British Columbia, Canada

Ogochukwu Judith Okakpu
Department of Pure and Industrial Chemistry, Nnamdi Azikiwe University, Awka, Nigeria

*Corresponding Author's Email: sm.ofochebe@unizik.edu.ng

ARTICLE INFO

Keywords: *Static Performance, Vertical Access Risers, Deepwater, Floating Production System*

Received: 18, Feb. 2026
Revised: 07, Mar. 2026
Accepted: 09, Mar. 2026

©2026 Author(s): This is an open-access article distributed under the terms of the Creative Commons Attribution 4.0 International

ABSTRACT

The requirements of marine risers applied to deepwater floating production systems become more and more challenging as oil/gas exploration and production continue to shift towards deeper waters. Compliant vertical access riser (CVAR) is a new riser concept being developed to address the potential challenges. Static analysis of the CVAR system is carried out in this study using a model developed from the differential equilibrium of the static forces, modified based on suspended cable theory and catenary equations. This study noted that the static performance of the CVAR system, evaluated in terms of the equilibrium position, the effective tension and the bending moment depends on the buoyancy factor (BF) and other secondary factors including the location of the buoyancy modules away from the wellhead and the degree of compliance. Keeping the BF value low as much as possible for a constant total riser length pushes the equilibrium location of the buoyancy modules to lower riser region, and increases the degree of compliance as well as the operational advantages.

INTRODUCTION

Since the last century, oil and gas exploration has continued to shift from onshore (shallow water) to deep water offshore locations in attempt to satisfy the growing demand for the products, in the face of depleting onshore reserves. The shift to deeper waters has come with considerable technological challenges. One of the major challenges is that rigid production platform is not feasible for ultradeep water operations, thus, the floating production system (FPS) is usually applied. The FPSs are more conservative in compatibility with production risers. Only compliant risers such as steel catenary risers (SCRs), lazy wave risers (LWRs), flexible risers (FRs) and hybrid risers (HRs) are used to support oil/gas transportation in deep-water floating FPSs, (Gonzalez et al., 2015; Buberg, 2014; Khan et al., 2011). Currently, exploration is taken deeper to water depth exceeding 3000 meters. However, these conventional risers are not convenient for FPSs operations in ultradeep water of depth exceeding 1500meters, due to their inherent limitations. As a result, a new riser concept called compliant vertical access risers (CVAR) is being developed to meet the requirements of FPSs

operation at ultradeep water field. The CVAR system has differentiated geometry characterised by three segments, the lower segment, the transition region and the upper segment (Lou, Hu, et al., 2019).

The lower segment and the upper segment are made to connect vertically to the wellhead and the production platform respectively. Buoyancy modules are spread from the upper part of the lower segment through the transition region to the lower part of the upper segment. By proper specification of the buoyancy factor at each segment and the total riser length, the transition region forms a spline wave such that the leading edge connects the lower riser segment and the trailing end connects the upper riser segment. This desirable geometry of the CVAR compensates for heave platform motion in a very economical way by maintaining vertical connection with the wellhead and the production platform, as well as a minimum offset distance between them. This unique feature of the CVAR system has some practical advantages that makes the system more appropriate for deepwater FPSs. For example, with proper specification of buoyance factors, the maximum axial riser tension is very low, compared to the conventional risers. Sophisticated subsea facilities are not required to keep the risers connected to the wellhead since the risers approached the wellhead from vertical direction. Moreover, workover operations can be carried out directly from the production platform during well interventions, instead of using a different platform due to reduced offset of the platform from the wellhead. These desirable attributes of the CVAR system amount to significant operational expediencies and cost savings.

Very few published researches have attempted to carry out static analysis of CVAR system using different methods. For instance, Lou, Hu, et al., (2019) established the static equilibrium position and axial tension for the CVAR system at water depth of 2438m, and applied the results for stability analysis of the CVAR system. However, the work focused on the stability analysis, thus necessary information about the mathematical formulation and the detailed procedure for the static analysis were not discussed in the article. In another closely related work, Lou, Li, et al. (2019) investigated the observable changes in the CVAR riser static configuration subjected to extreme drift conditions using finite element method. The later study established a far-end and near-end riser positions, relative to the equilibrium position. On this basis, further studies were carried out by the research team to monitor the effects of other parameters such as buoyancy factor (BF) and location of the buoyancy modules along the riser length on the mechanical response. The later study found that, while the degree of compliance and the BF should be kept moderate, the buoyancy modules should be placed in the lower region, in order to maximize the operational advantages of CVAR system. The present study noted that the buoyancy factor (BF) setting of the CVAR actually affects, not just the mechanical response as highlighted in the cited articles, but determines the equilibrium state generally; including the offset of the platform from the wellhead, the location of the buoyancy modules along the riser length, the axial tension/bending moment as well as the internal stress. Thus, further assessment of the static problems is carried out in the present study to reflect this reality

METHODOLOGY

The CVAR system is approximated to a cable with considerable bending stiffness, subjected to vertical and horizontal static loads, such as self-weight, buoyancy, hydrostatic pressure, current, floater movement (static offset). Then, the governing equation is derived from the differential equilibrium equations. To simplify the problem, the riser is first modelled as an inextensible cable without bending stiffness, subjected to effective weight, drag force and offset as shown in Figure 1. Later, the suspended cable equations are coupled to the classical catenary equations to evaluate the coordinates, the force components and account for the bending stiffness.

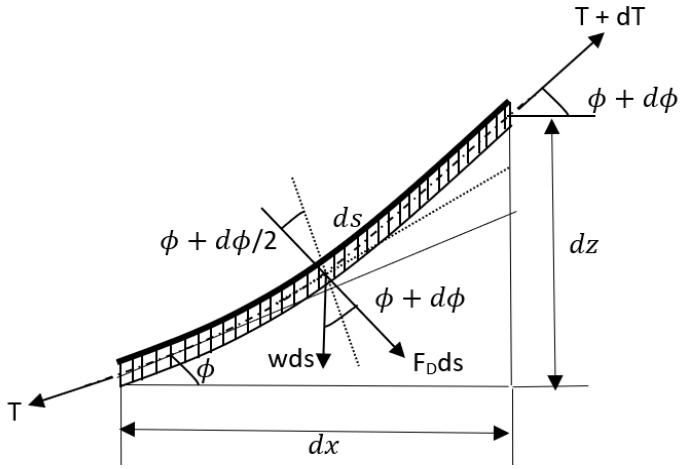


Figure 1: Static loads on a differential riser element

Equilibrium of forces acting on the differential riser segment (Figure 1) is expressed as:

$$(T + dT)cos(d\phi) - T - wsin(\phi + d\phi/2)ds + f_D sin(d\phi/2)ds = 0 \quad (1)$$

$$wcos(\phi + d\phi/2)ds + f_D cos(d\phi/2)ds - (T + dT)sin(d\phi) = 0 \quad (2)$$

Where But, $cos(d\phi) = cos(d\phi/2) \cong 1$, $sin(d\phi) \cong d\phi$, and $sin(d\phi/2) \cong d\phi/2$ for a small angle of inflection. Thus, ignoring higher order terms, the force balance equations become:

$$dT - wsin(\phi)ds = 0 \quad (3)$$

$$Td\phi - wcos(\phi)ds - f_D ds = 0 \quad (4)$$

From the geometry of the differential riser element

$$dx = ds\ cos(\phi) \quad (5)$$

and $$dz = ds\ sin(\phi) \quad (6)$$

The effect of the sea currents can be evaluated using the Morison equation (Lei et al. 2017) expressed for a horizontal current velocity (v), as:

$$f_D = \frac{1}{2}\rho C_d D v sin(\phi)\lceil vsin(\phi)\rceil \quad (7)$$

Thus, the system of equation for the static analysis is expressed as

$$\begin{cases} dT/ds = wsin\phi \\ d\phi/ds = \frac{1}{T}\left[wcos(\phi) + \frac{1}{2}\rho C_d D v sin(\phi)\lceil vsin(\phi)\rceil\right] \\ dx/ds = cos(\phi) \\ dz/ds = sin(\phi) \end{cases} \quad (8)$$

For the riser segment in contact with the seabed:

$$R_s = w \quad (9)$$

and $dT/ds = 0$ (10)

where R_s is the soil reaction and T is the effective tension, w is weight per unit length of the riser, and f_D represents the drag force.

Static configuration of the CVAR is obtained by integration equation (8), but before that is done, the force components and the coordinates are first evaluated in the local coordinate system, element by element, using the classical catenary equations and suspended cable equations as follows:

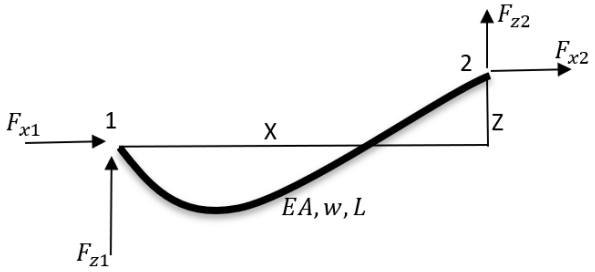


Figure 2: Definition of terms in catenary equation

For a typical line element characterized by node 1 and node 2 as shown in Figure 2, catenary equation established that (Leira, 2010):

$$F_{x2} = -F_{x1} \tag{11}$$

$$F_{z2} = -F_{z1} + wL \tag{12}$$

$$X = -F_{x1}\left[\frac{1}{EA} + \frac{1}{w} ln\left(\frac{F_{z2} + T_2}{T_1 - F_{z1}}\right)\right] \tag{13}$$

$$Z = \frac{1}{2EAw}(T_2^2 - T_1^2) + \frac{1}{w}(T_2 - T_1) \tag{14}$$

$$I_d = 1 + \frac{1}{2EAw}\left[F_{z2}T_2 + F_{z1}T_1 + F_{x1}^2 ln\left(\frac{F_{z2} + T_2}{T_1 - F_{z1}}\right)\right] \tag{15}$$

where

$T_1 = (F_{x1} + F_{z1})^{1/2}$ and $T_2 = (F_{x2} + F_{z2})^{1/2}$

While the suspended cable equations that govern the geometry of the riser suggest that for the conceptual 5-segments CVAR system studied:

$$L_1 = \left[\left(\frac{w_3 y_3}{w_1 - w_3}\right)^2 - \frac{2T_h w_3 y_3}{w_1(w_1 - w_3)}\right]^{1/2} \tag{16}$$

$$\beta_1 = w_1 L_1 / T_h \tag{17}$$

$$\beta_2 = \beta_1 + w_2 L_2 / T_h \tag{18}$$

$$\beta_3 = \beta_3 + w_3 L_3 / T_h \tag{19}$$

$$\beta_4 = \beta_3 + w_3 L_3 / T_h \tag{20}$$

$$\beta_5 = \beta_3 + w_3 L_3 / T_h \tag{21}$$

$$z_5 = \frac{T_h}{w_3}\left(\sqrt{1 + \beta_5^2} - \sqrt{1 + \beta_4^2} - \sqrt{1 + \beta_3^2}\right) \tag{22}$$

$$z_4 = \frac{T_h}{w_3}\left(\sqrt{1+\beta_4^2} - \sqrt{1+\beta_3^2}\right) \quad (23)$$

$$z_3 = \frac{T_h}{w_3}\left(\sqrt{1+\beta_3^2} - 1\right) \quad (24)$$

$$y_3 = z_l - z_3 - z_4 + z_5 \quad (25)$$

where L_1 is the length of bare (unbuoyed) lower riser segment. L_2, L_3 and L_4 are lengths of the buoyed sections of the lower segment, the transition zone and the upper segment respectively, while L_5 is the length of the unbuoyed upper riser segment. β is the angle with which a segment connects the next segment measured at the intersection with respect to the horizontal line. T_h is the horizontal tension force. A MATLAB program is written to integrate equation (8) subject to the function definitions provided by the catenary and the suspended cable equations.

RESULTS

The basic parameters of the CVAR system suggested by Mungall et al. (2004) is adopted as a basis for the static analysis. The specific parameter values are presented in Table 1. The static analysis is tailored to determine the effects of buoyancy factor (BF) and riser overlength fraction (OF) settings on some performance functions of the CVAR system including the riser geometry, the axial tension and the bending moment.

Table 1: Fixed parameters of the CVAR (Lou, Hu, et al., 2019)

Riser property	Symbol	Value
Outside diameter	D	0.3m
Wall thickness	WT	0.038
Water depth	zL	2438m
Elastic modulus	E	2.07×10^{11}Pa
Added mass coefficient	C_a	1
Drag coefficient	C_d	1
Material density	ρ_m	7850kg/m^3
Seawater density	ρ_w	1025 kg/m^3
Density of internal fluid	ρ_f	800 kg/m^3
Acceleration due to gravity	g	9.807m/s^2

3.1 Position analysis

Using the data about the CVAR shown in Table 1, and the proposed method described in section 3.0, the position chart is evaluated at some specified conditions and the result is presented in Figure 3. Two practical approaches to the statics problem are considered. In the first approach, the total riser length is assumed constant at 2601m, the buoyed segments lengths $L_2(=190m), L_3(=416m)$ and $L_4(=88m)$ are assumed constant and contiguous, the buoyancy factors of the transition zone (BF_2) and the upper segment (BF_3) are maintained at 2 and -1.4 respectively, while the that of the lower riser region (BF_1) is varied in a valid space of 6 – 12. The equilibrium position of the CVAR is found for the various cases of adjustments of BF_1 at different locations of the buoyancy modules along the riser length as shown in Figure 3. The observed trend shows that as BF_1 value is increased from 6 - 12, the equilibrium position of the buoyancy modules measured from the touch down point (TDP) labelled L_1, increased from 315m to 1061m. This resulted in corresponding increase in the static offset of the anchor point from 570 – 660m with respect to the TDP. The best

position that addressed the need to keep the offset of the anchor point closer to the wellhead is achieved at $BF_1 = 6$. Efforts to evaluate the position of the system at other range of $BF_1 < 6$ (or > 12) yielded invalid results.

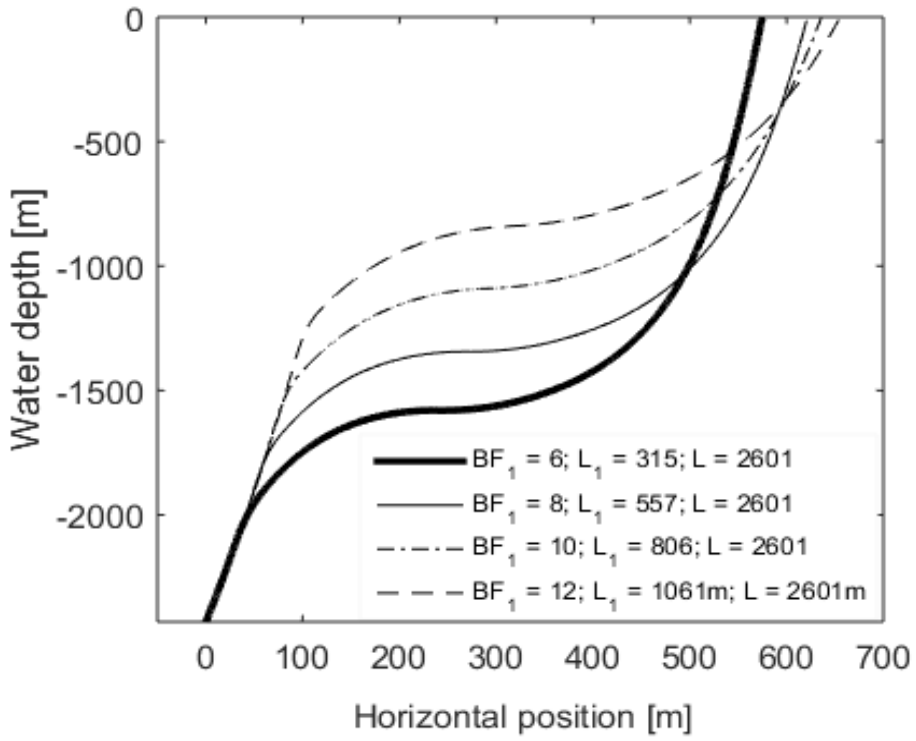


Figure 3: Equillibrium position of the CVAR obtained for a fixed riser length at various buoyancy factor setting

3.2 Axial tension/bending moment

To investigate further the rationality of the buoyancy factor setting, the effective tension of the riser is evaluated at specific values of BF_1. The results are presented in Figure 4. From the result, the tensions at the TDP and the hang off point are generally higher than the tension at the transition zone due to the effects of the buoys. As BF_1 is increased from 6 – 10, the tension at the lower riser segment and transition zone increased uniformly, the tension at the upper section also increased, but at a reduced rate. In other words, attempts to allow for increased length of the bare lower riser segment, L_1 associated with increased value of BF_1 result in rising tension in the lower riser segment. At some points, the effective tension at the TDP exceeds that of the anchor point which is not desirable. In the lower bare riser region, maximum tension is witnessed in each case at the intersection of the buoyant region. The general trend suggests that the most desirable riser tension is also obtained at $BF_1 = 6$.

The effects of the buoyancy factor setting on the bending moment of the riser is shown in Figure 5. The results indicate that maximum bending moment is witnessed in each case at the transition region. The system with BF_1 value of 6 recorded maximum bending moment at the transition zone, making it more susceptible to failure from high bending stress. The peak bending moment reduced progressively as BF_1 value was increased from 6 to 10. The trend suggests that a detailed stress analysis of the system is required to justify the choice of the buoyancy factor setting in the studied range. Reduction in the peak bending moment/stress value, with less than 80m predicted increase in the static offset of the anchor point achieved towards higher BF_1 values appears quite

desirable, but the effects of the associated rising tension, especially in the lower riser region and the transition zone must be considered. In a detailed design-optimization of the system, efforts would be made to reach a compromise between the needs for a reduced static offset of the anchor point from the wellhead/low riser tension obtainable at low value of $BF_1 = 6$, and low bending stress/increase static offset of the anchor point, obtainable at higher BF_1 values.

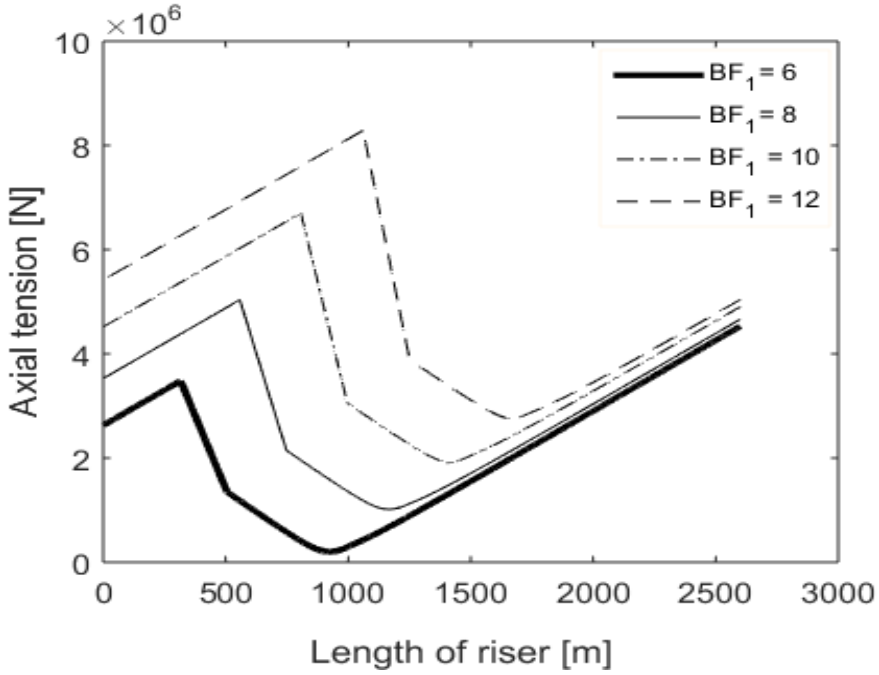


Figure 4: Effective tension of the CVAR obtained at various buoyancy factor setting

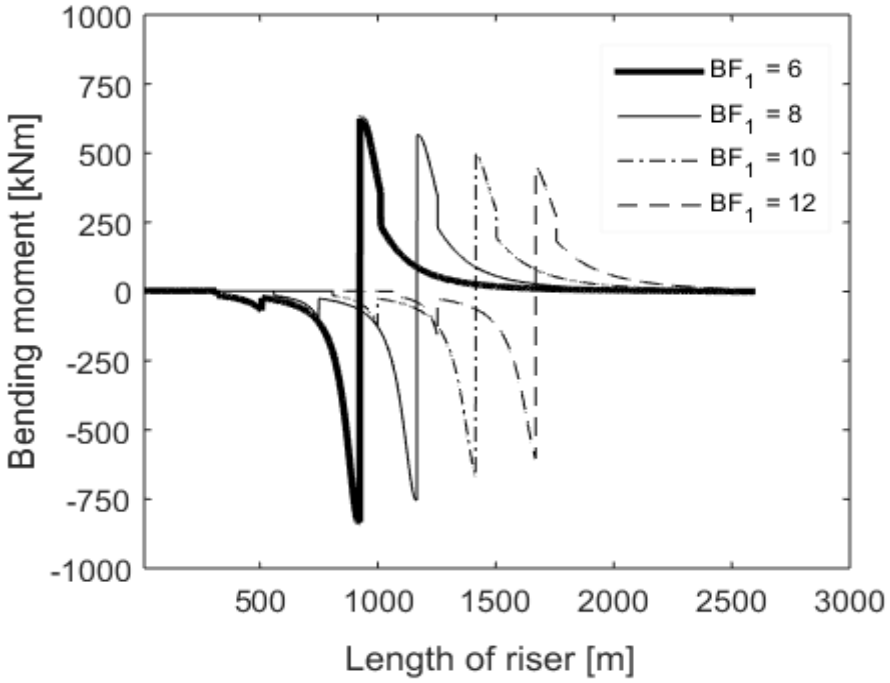


Figure 5: Bending moment of the CVAR obtained at various buoyancy factor setting

3.3 Combined Effects of Buoyancy Factor and Riser Overlength on the Equilibrium of the CVAR

Another approach to the static analysis is to consider the total riser length, L together with the buoyancy factor (BF) of the riser as free variables, while the equilibrium condition of the system is evaluated. In this approach, it is found that the geometric rise in tension of the lower riser region witnessed at higher BF_1 values for a constant riser length is avoided using increased riser overlength. The position chart obtained at equilibrium condition as BF_1 is varied in a space of 6 – 12 (allowing for increased riser overlength) is presented in Figure 6. The total length of risers at equilibrium condition increased from 2601m at $BF_1 = 6$ to 4770m at $BF_1 = 12$.

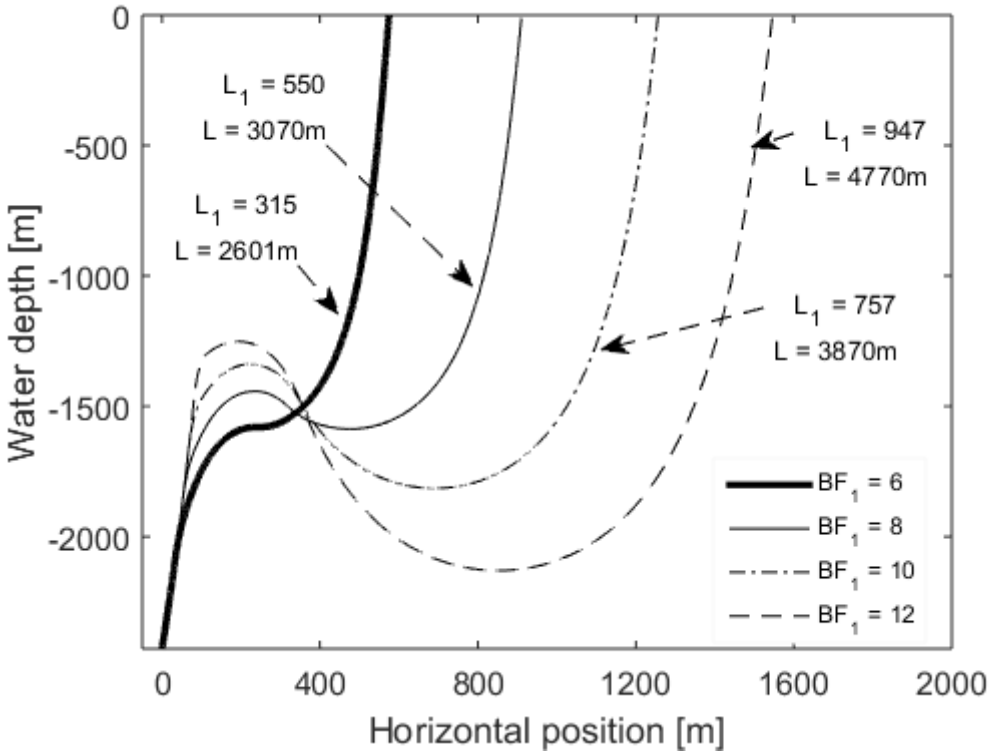


Figure 6: Vertical position chart of the CVAR obtained within a valid range of buoyancy factor setting of the lower riser region

One can understand from the result that the system with $BF_1(= 6)$ yielded apparently more desirable geometry by providing, reduced total riser length of 2601m and shortest horizontal offset of the anchor point from the wellhead < 600m. Riser overlength was progressively increased as the BF_1 value increased from 6 – 12. This resulted in increased offset of the anchor point. Comparing the results on the riser tension with those obtained from the first analysis approach as shown in Figure 7(a) and Figure 7(b), it becomes clearer that operating the system with increased riser overlength moderates the riser tension. Maximum riser tension of about 5500kN is obtained at the lower riser segment with $BF_1 = 12$, compared to the peak tension value above 8000kN obtained at the same point, in the case of fixed riser length. The riser tensions at the TDP and the anchor point are not significantly affected by the BF_1 value at equilibrium condition.

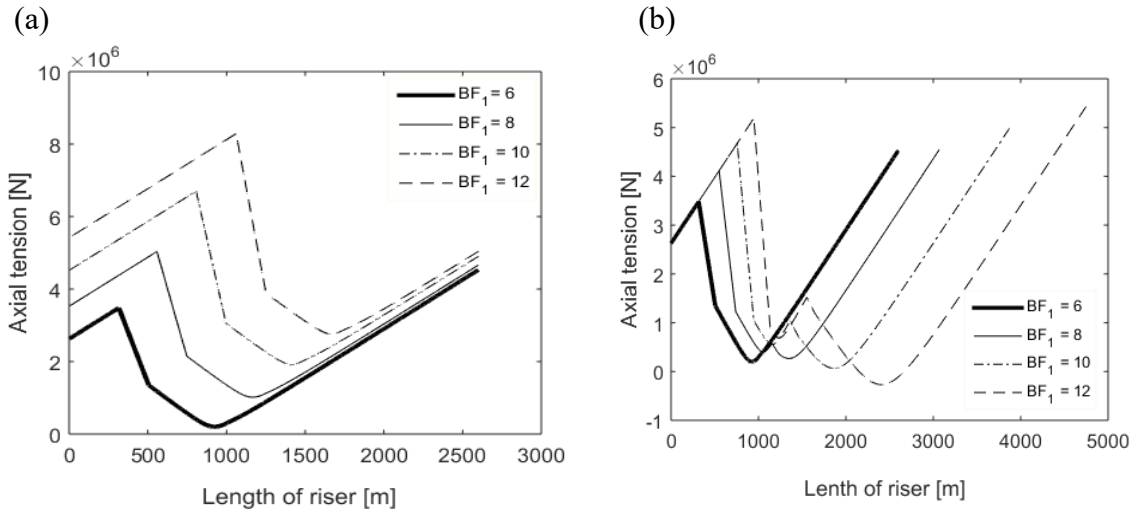


Figure 7: Axial tension of the CVAR obtained at specific BF_1 values compared between; (a) the constant total riser length system and (b) the variable total riser length system

Although, the tension at the TDP is not significantly affected by the value of BF_1 in the valid range, the peak tension in the lower riser region increased together with the local and the total riser length at higher BF_1 values. The result further reveals the tendency of reaching a negative tension (or greater compression) of the riser around the transition region with higher BF_1 value. Worse cases of this scenario observed at BF_1 value > 12 lead to twisting of the risers. The axial riser tension at the touch down point is fixed at 2500kN and the axial tension at the anchor points is found in the range of 4500 – 5500kN, depending on the total riser length.

The static bending moment diagram of the CVAR system compared between the alternative analysis approaches in Figure 8(a) and Figure 8(b) shows that the peak bending moment of the CVAR at higher BF_1 values approached that of BF_1 = 6, in the negative axis due to increasing riser overlength.

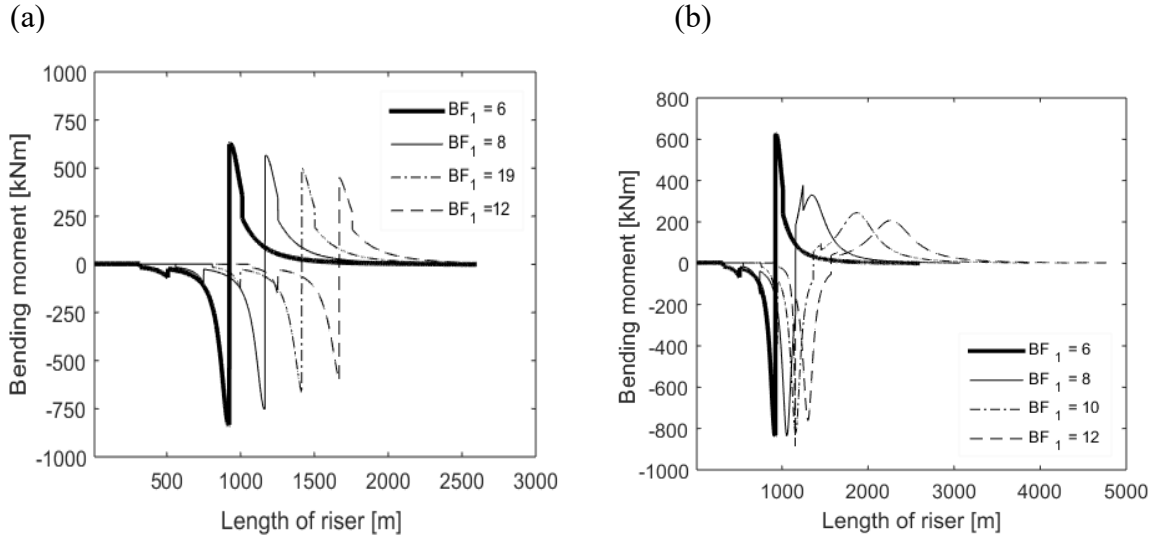


Figure 8: Bending moment of the CVAR obtained at various BF_1 values compared between (a) the constant total riser length system and (b) the variable total riser length system

The locations of the minimum and the maximum bending moments apparently coincided, in each case, with the leading edge of the gravity block and its boundary with upper region, respectively.

The minimum and maximum bending moments occurring within a very close range assisted in the formation of a desirable riser geometry. For the same reason, the buoyancy factors BF_2 and BF_3 of the transition and the upper section were kept constant during the investigations. The system with BF_1(=6) shows significantly high peak bending moment due to reduced riser overlength and low radius of curvature at the transition zone. The overall trend suggests that, although the system with BF_1(=6) shows desirable geometry and reduced axial tension at equilibrium condition, yet, it is prone to greater material stress and fatigue failure at the transition zone. In other words, a detailed stress analysis is needed to justify the selection of a suitable buoyancy factor.

CONCLUSION

The major conclusions of this study are

i. Static performance of the compliant vertical access riser (CVAR) system measured in terms of the equilibrium position, the axial tension and the bending moment is primarily affected by the buoyancy factor (BF).
ii. The minimum total length of risers and offset distance required to operate the proposed CVAR system at nominal water depth of 2438m is 2601m and 520m respectively. This is equivalent to 0.0434 degree of compliance.
iii. Buoyancy factor specification of 6, 2 and -1.5 at the lower segment, the transition zone and the upper segment, respectively yielded the most desirable anchor offset position (=520m) and improved axial tension for the proposed CVAR system, while improved bending moment is obtainable towards higher BF values.
iv. To reach a compromise between the requirements for a reduced axial tension/anchor position offset and low bending moment which are opposed to each other, a detailed stress analysis and optimization study of the CVAR system are required.

REFERENCES

Buberg, T. (2014). *Design and Analysis of Steel Catenary Riser Systems for Deep Waters* (Issue June). Norwegian University of Science and Technology.

Gonzalez, G. M., De Sousa, J. R. M., & Sagrilo, L. V. S. (2015). An Unbonded Flexible Pipe Finite Element Model. *Proceedings of the XXXVI Iberian Latin American Congress on Computational Methods in Engineering*, *April 2016*. https://doi.org/10.20906/cps/cilamce2015-0373

Khan, R. A., Kaur, A., Singh, S. P., & Ahmad, S. (2011). Nonlinear dynamic analysis of marine risers under random loads for deepwater fields in Indian offshore. *Procedia Engineering*, *14*, 1334–1342. https://doi.org/10.1016/j.proeng.2011.07.168

Lei, S., Zhenga, X. ., & Kennedy, D. (2017). Dynamic response of a deepwater riser subjected to combined axial and transverse excitation by the nonlinear coupled model. *International Journal of Non-Linear Mechanics*, *97*, 68–77.

Leira, B. J. (2010). *Review and verification of marine riser analysis programs : Global response analysis*. Norwegian University of Science and Technology.

Lou, M., Hu, P., Qi, X., & Li, H. (2019). Stability analysis of deepwater compliant vertical access riser about parametric excitation. *International Journal of Naval Architecture and Ocean Engineering*, *11*(2), 688–698. https://doi.org/10.1016/j.ijnaoe.2019.02.005

Lou, M., Li, R., Wu, W., & Chen, Z. (2019). Static performance analysis of deepwater compliant vertical access risers. *International Journal of Naval Architecture and Ocean Engineering*, *11*(2), 970–979. https://doi.org/10.1016/j.ijnaoe.2019.04.007

Mungall, C., Haverty, K., Bhat, S., Andersen, D., Sarkar, I., & Wu, J. (2004). Semi- submersible Based Dry Tree Platform with Compliant Vertical Access Risers. *Offshore Technology Conference, Pp. 1e13.*